Universal Behavior of Membranes with Sterols

J. Henriksen,* A. C. Rowat,* E. Brief,† Y. W. Hsueh,‡ J. L. Thewalt,†§ M. J. Zuckermann,† and J. H. Ipsen*
*MEMPHYS - Centre for Biomembrane Physics, Department of Physics, Syddansk Universitet, Odense, Denmark; †Department of Physics, Simon Fraser University, Burnaby, British Columbia, Canada; ‡Department of Physics, National Central University, Chungli, Taiwan; and §Department of Biochemistry and Molecular Biology, Simon Fraser University, Burnaby, British Columbia, Canada

ABSTRACT Lanosterol is the biosynthetic precursor of cholesterol and ergosterol, sterols that predominate in the membranes of mammals and lower eukaryotes, respectively. These three sterols are structurally quite similar, yet their relative effects on membranes have been shown to differ. Here we study the effects of cholesterol, lanosterol, and ergosterol on 1-palmitoyl-2-oleoyl-*sn*-glycero-3-phosphatidylcholine lipid bilayers at room temperature. Micropipette aspiration is used to determine membrane material properties (area compressibility modulus), and information about lipid chain order (first moments) is obtained from deuterium nuclear magnetic resonance. We compare these results, along with data for membrane-bending rigidity, to explore the relationship between membrane hydrophobic thickness and elastic properties. Together, such diverse approaches demonstrate that membrane properties are affected to different degrees by these structurally distinct sterols, yet nonetheless exhibit universal behavior.

INTRODUCTION

Among the vast diversity of components in biological membranes, sterols are one of the most abundant constituents and are found in a wide range of membranes across various species. To name a few, cholesterol predominates in the plasma membrane of mammalian cells, whereas ergosterol is the major sterol in the membranes of lower eukaryotes including some protozoa, yeast, fungi, and insects such as *Drosophila*. Lanosterol is the most abundant sterol in some prokaryotic membranes and is the biosynthetic precursor of cholesterol and ergosterol. The overall morphology of these three molecules is similar, but they exhibit small structural differences (Fig. 1). Why there is such variation throughout the evolution of sterol structure and the consequences for biological function remains unresolved. This question has motivated membrane researchers to explore the topic of sterols in biological membranes for over 30 years. Sterols are known to affect short- and long-range membrane order, protein function, and cell growth (1,2). The role of sterols in biosynthesis is well understood and the pathways of sterol synthesis and membrane evolution have been correlated (3–5). However, the advantage that particular sterols provide for certain species is not clear. The fact that sterols are potent modulators of membrane physical properties indicates that these molecules may be of major significance for the function and evolution of the biological membrane (6).

Our understanding of sterol-lipid mixtures has developed from extensive studies of cholesterol-lipid mixtures using a variety of biophysical techniques (1,7–14). Based on experimental results, a theoretical description (10,15) captured the essence of cholesterol's effects on membranes: cholesterol disrupts the lateral order of the gel phase (s_o), tends to order the liquid phase (l_d), and at higher cholesterol content, stabilizes a new phase, the liquid-ordered phase (l_o). This l_o phase exhibits both rapid transverse diffusion and translational disorder of the liquid-disordered phase (l_d) and relatively ordered lipid chains characteristic of the solid-ordered phase (s_o). The overall topology of the obtained phase diagram for binary lipid-cholesterol mixtures has been shown to hold for a range of PC-lipids with both saturated and monounsaturated acyl chains (10,11,16–19), including POPC-cholesterol mixtures (19–21). Lanosterol and ergosterol have also been found to promote acyl-chain order at higher concentrations (14,22). Comparative studies of these three sterols have been conducted (13,23,24) and reveal, despite their structural similarities, differences in the effect of cholesterol, lanosterol, and ergosterol on membrane properties.

How sterols affect membranes has been experimentally investigated on both mesoscopic and macroscopic scales. In particular, deuterium nuclear magnetic resonance (^{2}H-NMR) is well suited for studying mesoscopic membrane properties (~1–100 nm). Using lipids with perdeuterated acyl chains, ^{2}H-NMR can reveal details of lipid acyl conformation, orientational order, and dynamics. Whereas ^{2}H-NMR is sensitive to changes in bilayer properties on a molecular scale, micromechanical techniques, such as micropipette aspiration and vesicle fluctuation analysis (VFA), provide access to global membrane properties. Both ^{2}H-NMR and micromechanical techniques have been used to investigate how sterols induce changes in membrane properties. These studies have demonstrated that cholesterol has a significant ordering effect on acyl chains (6,14,21,25–27) and increases membrane mechanical stability (13,28–33). Lanosterol (14,23) and ergosterol (22,23) have also been determined to order lipid acyl chains and increase membrane stability

Submitted June 3, 2005, and accepted for publication October 6, 2005.

Address reprint requests to J. H. Ipsen, Tel.: 45-6550-2560; E-mail: ipsen@memphys.sdu.dk.

0006-3495/06/03/1639/11 $2.00

doi: 10.1529/biophysj.105.067652

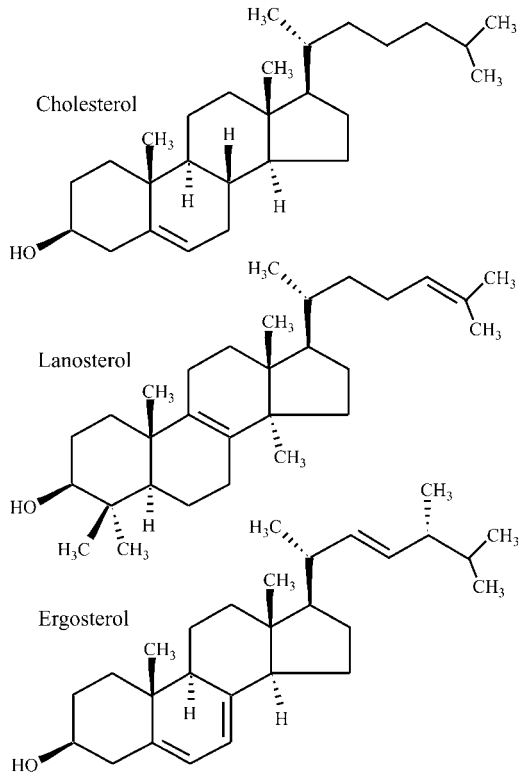

FIGURE 1 Structures of cholesterol, lanosterol, and ergosterol. In the biosynthetic pathway, the methyl groups on lanosterol's α-face are shed, giving rise to cholesterol. Ergosterol differs structurally from cholesterol in that it has two additional double bonds as well as a methyl group on the side chain.

(33). Correlating the results obtained from the two techniques has been pursued (13). However, a detailed understanding of how the fundamental interactions between sterols and lipids give rise to global changes in membrane properties is lacking.

Here we investigate mixtures of cholesterol, lanosterol, and ergosterol in POPC lipid membranes at room temperature using both micropipette aspiration and ^{2}H-NMR. Micropipette aspiration experiments reveal that all three sterols increase the area expansion modulus, K_a, of POPC membranes. These results are correlated to values of membrane-bending rigidity, κ, that we previously determined using VFA (33). We show that the mechanical moduli, K_a and κ, correlate with the first moments, M_1, of the spectra obtained by ^{2}H-NMR. Taken together, our results demonstrate that cholesterol, lanosterol, and ergosterol are potent membrane rigidifiers in terms of both area compressibility and bending moduli. The ability of these sterols to order lipid acyl chains is demonstrated in the observed increase in the average ^{2}H-NMR order parameter (M_1). For POPC membranes, this ordering effect follows the sequence cholesterol $>$ lanosterol $>$ ergosterol. Relating K_a and κ to M_1 reveals that membrane mechanical properties are modulated by bilayer hydrophobic thickness and demonstrates how sterol-induced molecular order manifests on a mesoscopic scale. Ultimately, this integrated approach combining diverse experimental techniques and theory provides a deeper understanding of fundamental sterol-lipid interactions, and also reveals universal characteristics of membrane order and mechanics that probably extend beyond lipid-sterol mixtures.

MATERIALS AND METHODS

Micropipette aspiration

A physical description of the mechanical deformations of a fluid lipid vesicle is embedded in Helfrich's curvature free energy (34),

$$\mathcal{H} = \frac{K_a}{2A_0}(A - A_0)^2 + \frac{\kappa}{2}\int (2H - C_0)^2 \, dA, \qquad (1)$$

where the first term represents the elastic energy associated with in-plane dilation of the membrane area, A. The equilibrium area and area expansion modulus are given by A_0 and K_a. The second term is the Helfrich bending energy that describes out-of-plane shape changes. Here H is the mean curvature, C_0 is the spontaneous curvature ($C_0 = 0$ for a symmetric bilayer) (34), and κ is the bending rigidity. Typical values of these material parameters for single-component fluid lipid membranes are $K_a = 0.1 - 1$ J/m^2 = 20–200 k_BT/nm^2 and $\kappa = 10 - 100$ k_BT (35).

The micropipette aspiration technique allows for determinations of both K_a and κ. In such an experiment, a giant unilamellar vesicle is manipulated by the use of a micropipette (Fig. 2 *a*). During the course of an aspiration cycle, the vesicle is gradually pressurized by applying an aspiration pressure, Δp. This leads to a progressive increase in the projection of the vesicle, L, inside the pipette of radius R_1 (Fig. 2 *b*). The response to aspiration pressure exhibits a nonlinear form: in the low-pressure regime, there is a logarithmic relationship between aspiration pressure and L, whereas at higher aspiration pressures, the relationship is linear (36–38). Typically, values of κ are extracted at low pressures and K_a at higher pressures. In the high-pressure regime ($\Delta p \geq 10^3$ Pa), the membrane's microscopic area dilates in response to the in-plane tension, and analysis of the linear Hookean elastic response yields an estimate of K_a. We previously reported κ-values for sterol-lipid membranes determined by VFA, so we focus in this study on the determination of K_a. In a recent study (37), we have demonstrated full agreement between estimates of κ obtained by the micropipette aspiration technique and VFA. The vesicle yield is much higher with VFA than the micropipette aspiration technique, so we will rely on the previously reported values of κ for sterol-lipid membranes determined by VFA (39) and in this study focus on the determination of K_a.

Sample preparation for micropipette aspiration

POPC and cholesterol (98% pure) were obtained from Avanti Polar Lipids (Birmingham, AL), lanosterol (~97% pure), and solvents from Sigma-Aldrich (Copenhagen, Denmark), and ergosterol (≥97% pure) from Fluka (Buchs, Switzerland). Purity of the sterols was verified by thin-layer chromatography (TLC) as previously described (33). Due to inhomogeneous mixing, methanol alone, rather than methanol/chloroform (MeOH:$CHCl_3$), was chosen as solvent for the lipid-cholesterol mixture (11). To achieve solubility, lanosterol and ergosterol were dissolved in 1:9 MeOH:$CHCl_3$ and 1:3 MeOH:$CHCl_3$. Solutions of ~0.1–0.3 mg(POPC)/ml containing 10, 20, and 30 mol% sterols were prepared and 10 μl of the lipid/sterol mixture was deposited on platinum wire electrodes. After evaporation overnight in a vacuum chamber, giant unilamellar vesicles were formed by electroformation (40,41) in a 250 mOsm sucrose solution. Vesicles were resuspended in a 250 mOsm glucose solution contained in the thermostated observation chamber. A freezing-point osmometer (Model 3D3, Advanced Instruments, Norwood, MA) was used to regulate solution osmolarities and Milli-Q water was used

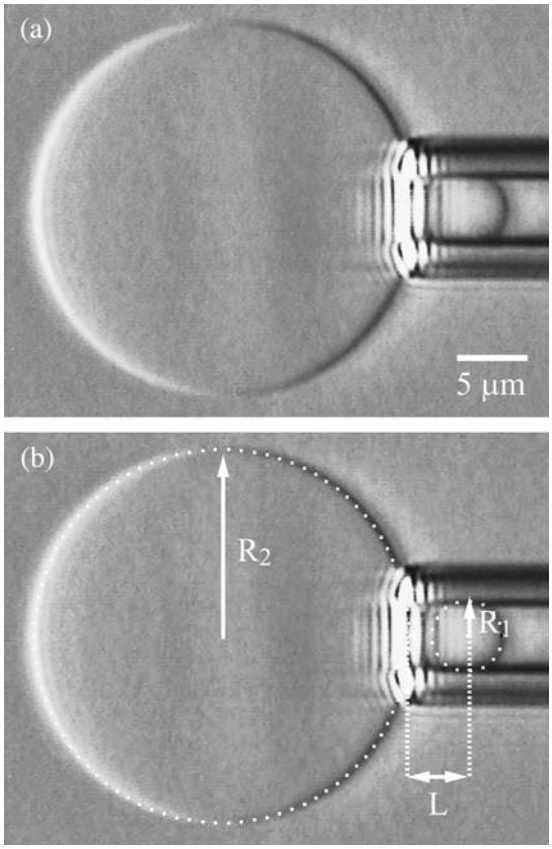

FIGURE 2 Images showing an aspirated vesicle (diameter $\simeq$40 μm) in the high-pressure regime: (*a*) the raw image and (*b*) the analyzed form. From the analysis (described in (37)), the radius of the outer sphere, R_2, the length of the cylinder, L, and the pipette radius R_1 are determined.

throughout (Millipore, Bedford, MA). Samples were prepared from a homogeneous mixture of lipids and sterols, and considering the rapid transbilayer diffusion exhibited by cholesterol (42), it is reasonable to assume a homogeneous distribution of sterols in both monolayers.

Micropipette setup

Aspiration measurements were conducted on an inverted microscope (Zeiss Axiovert S100, Göttingen, Germany), equipped with Hoffman modulation optics (HMC 40 LWD 0.5 NA infinity-corrected objective, GS 40 mm w.d. 0.6 NA condenser). Images were acquired using a charge-coupled device camera (Model SSC-DP50AP, Sony, Tokyo, Japan) connected to a PC through a framegrabber (Sigma-SLC, Matrix Vision, Oppenweiler, Germany). Micromanipulators were used to position the pipette. The micropipettes were pulled from 1-mm-diameter capillaries and were treated before use with a 1 mg/ml bovine serum albumin (99% essentially fatty-acid-free, Sigma-Aldrich) solution to prevent membranes from adhering to the pipette. Pressures in the range 10^3–10^4 Pa were applied and measured using a pressure transducer (DP1530/N1S4A, Validyne, Northridge, CA).

Aspiration experiments were conducted in a thermostated chamber (25°C) with open sides allowing for the entry of the micropipette. Vesicles were initially pre-stressed at a tension level of 2–4 mN/m to remove any internal lipid reservoirs in the form of buds or tubes. After a period of time ($\sim$60 s) the pressure was reduced to a level corresponding to $\sim$1 mN/m and then stepwise-increased. At each pressure level, a snapshot was recorded for analysis of vesicle geometry. The duration of an average aspiration experiment of a single vesicle was $\sim$5 min.

Micropipette data analysis

Here we present a modified version of the data analysis procedure presented in Henriksen and Ipsen (37) that we use to determine K_a. This is achieved by analyzing the change in optically resolved membrane area with respect to the equilibrium area in response to aspiration pressure. In the conventional data analysis procedure by Evans et al. (28,30), membrane deformation is described by the relative change in the optically resolved area, $\alpha = (A_p - A_p^{in})/A_p^{in}$, where A_p^{in} is the optically resolved area of the initial state. The optically resolved area of the aspirated vesicle is determined by approximating the mean shape of the vesicle as a hemisphere with a radius equal to the pipette radius, R_1, a cylinder of length L, and an outer sphere of radius, R_2,

$$A_p = 2\pi R_2^2\left(1 + \sqrt{(1 - (R_1/R_2)^2)}\right) + 2\pi R_1 L + 2\pi R_1^2. \tag{2}$$

The frame tension, τ, is the thermodynamic conjugate of A_p, and is, to a good approximation, related to the aspiration pressure (36,37),

$$\tau = \frac{R_1 \Delta p}{(1 - R_1/R_2)}. \tag{3}$$

The calculation of α assumes conservation of vesicle volume, a condition which is not strictly fulfilled (note that solvent evaporation from the chamber may account for drifting of the vesicle volume at 25°C) (37). Changes in volume are slow, thus the vesicle can be considered quasi-static throughout the duration of a single aspiration experiment and Eq. 3 is a reasonable approximation. We previously described image analysis of the vesicle's mean shape so that membrane deformations can be characterized without assuming constant volume (as shown in Fig. 2 *b*) (37).

Experimentally, we can access only the optically resolvable area (Fig. 2 *a*). Thus, the total membrane area cannot be resolved due to membrane undulations on suboptical length scales. As a consequence, K_a of the true membrane surface cannot be determined from the experimental observables alone in the high-pressure regime (37). However, K_a can be estimated by an apparent area expansion modulus, $\bar{K}_a$, that quantifies the response of the optically resolvable area to an increase in the membrane tension. The apparent area expansion modulus is defined as

$$\bar{K}_a = A_{p,0}\left(\frac{\partial \tau}{\partial A_p}\right)_T, \tag{4}$$

where the reference state, $A_{p,0} = A_p(\tau = 0)$, is the optically resolvable area at zero frame tension. A linear fit of $\tau \simeq (\partial\tau/\partial A_p)A_p - \bar{K}_a$ yields the apparent area expansion modulus (Fig. 3). The reference state, $A_{p,0}$ (Eq. 4) is uniquely defined by extrapolation of the optically resolvable area to zero frame tension (Fig. 3).

In the high-pressure regime, where $\bar{K}_a$ is determined, membrane undulations are greatly reduced but still persist. The correction due to the renormalization of K_a is described in Appendix 1. For these particular sterol-lipid systems, the relative reduction of the apparent area expansion modulus, $(\bar{K}_a/K_a - 1)$, is estimated to be 3–7% (see Eq. 18). Since this shift is modest, we present the uncorrected $\bar{K}_a$.

Values for $\bar{K}_a$ are each based on a population of 15–25 vesicles from at least two independent aspiration experiments. For each measurement it is possible that the vesicle is either multilamellar or has membrane defects, tethers, or buds that contribute to membrane area upon aspiration. Each population is statistically tested (Student's *t*-test) and aberrant vesicles emerge in the data population as distinct points that are removed. With this procedure, reliable estimates of $\bar{K}_a$ can be obtained to within $\sim$2%. This represents a major reduction in error on $\bar{K}_a$ determined by conventional micropipette analysis. Furthermore, this method of data analysis is much more efficient and does not require that vesicle volume remain constant—which is especially useful for experiments at higher temperature where solvent evaporation from the chamber can occur.

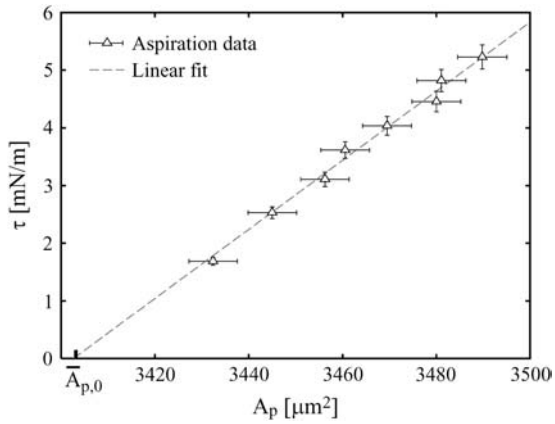

FIGURE 3 Plot of the data obtained from micropipette aspiration of a POPC lipid vesicle in the high-tension regime at 25°C. The data is presented in the form of the frame tension, τ (Eq. 3), as a function of the optically resolvable area, A_p (Eq. 2). The fitting range is limited to $\tau \geq 2$ mN/m, which yields the apparent area expansion modulus $\bar{K}_a = 204\,\mathrm{mJ/m^2}$. The error bars are estimated by $(\delta\tau/\tau) \sim (\delta R_1/R_1) \sim 1/25$ and $(\delta A_p/A_p) \sim (\delta R_2/R_2) \sim 1.5 \times 10^{-3}$. The zero frame tension area, $A_{p,0}$, is the intercept of the fitted linear curve and the x axis.

^{2}H-NMR

A membrane consisting of lipids with deuterated acyl chains gives rise to a ^{2}H-NMR spectrum that is a superposition of Pake doublets from deuterons at positions along the lipid acyl chains. The Pake doublets are distinguished by a quadrupolar frequency splitting that is proportional to the degree of conformational order along the lipid chain. As motions faster than the NMR timescale (10^{-6}–10^{-3} s) reduce the average quadrupolar splittings, the shape of the resulting frequency spectrum reflects acyl-chain conformation and dynamics. In the liquid crystalline phase that is characterized by rapid axially symmetric molecular motions, the quadrupolar splittings vary along the acyl chain due to the gradient in molecular motion characteristic of the fluid phase lipid bilayer. Below the main phase transition temperature, lipid chains become more constrained in their motions. The reduced, nonaxially symmetric chain motions are reflected in larger linewidths of each individual quadrupolar doublet and a wider spectrum characteristic of the gel phase. In this way, a ^{2}H-NMR spectrum reflects membrane phase behavior and acyl-chain order.

NMR sample preparation

POPC-d_{31} was obtained from Avanti Polar Lipids. Lanosterol (~97% pure), ergosterol (79% pure), and deuterium-depleted water were from Sigma-Aldrich Canada (Oakville, ON).

Multilamellar dispersions, typically of 80 mg POPC-d_{31} containing 0, 10, 20, and 30 mol % sterol, were prepared from mixtures of appropriate quantities of lipid and sterol in benzene/methanol (4:1, v/v). After freeze-drying, samples were rehydrated in a buffer containing 150 mM NaCl, 50 mM HEPES, 4 mM EDTA, and deuterium-depleted water (pH 7.4). Hydration was performed by freeze-thaw-vortex cycling five times between liquid nitrogen and 50°C. Samples were then transferred to NMR tubes and sealed. Before data acquisition, samples were equilibrated at 25°C for 2 h.

^{2}H-NMR spectra

^{2}H-NMR spectra were acquired using the quadrupolar echo technique (43) at 46.8 MHz. A typical spectrum resulted from 10,000–15,000 repetitions of the two-pulse sequence with 90° pulse length of 3.95 μs, interpulse spacing of 40 μs, and dwell time of 2 μs. The delay between acquisitions was 300 ms and data were collected in quadrature with Cyclops 8-cycle phase cycling. All spectra were obtained at 25°C.

Determining the first moments

The first moment, M_1, is a reflection of the average quadrupolar splitting and is defined as

$$M_1 = \frac{1}{2}\frac{\int_{-\omega_L}^{+\omega_L} f(\omega)|\omega|\,d\omega}{\int_{-\omega_L}^{+\omega_L} f(\omega)\,d\omega}, \tag{5}$$

where ω is the frequency shift from the central (Larmor) frequency, $f(\omega)$ is the spectral intensity, and $\pm\omega_L$ are the frequency limits of the spectrum. M_1 is related to the average order parameter by

$$M_1 \propto \frac{e^2qQ}{h}\langle|S_{CD}|\rangle, \tag{6}$$

where $S_{CD}(n) = (1)/(2)\langle 3\cos^2(\theta_n) - 1\rangle$, θ_n is the angle between the C–D bond of the n^{th} carbon position and the axis of symmetry of rapid motion of the acyl chain, and e^2qQ/h is the static quadrupolar coupling constant.

RESULTS

Micropipette aspiration

Table 1 and Fig. 4 display values obtained for the apparent area expansion modulus, $\bar{K}_a$. As shown, the presence of cholesterol, lanosterol, and ergosterol in POPC membranes induces an increase in $\bar{K}_a$ following the sequence cholesterol > lanosterol > ergosterol for all measured concentrations. For cholesterol and lanosterol, $\bar{K}_a$ increases monotonically as a function of sterol content whereas the effect of ergosterol levels off above 20 mol%. The relative increases in $\bar{K}_a$ for 10, 20, and 30 mol% sterol measured with respect to the value of pure POPC at 25°C are: 13%, 30%, and 66% for cholesterol; 8%, 22%, and 32% for lanosterol; and 2%, 9%, and 13% for ergosterol.

TABLE 1 Effects of sterols on POPC membranes at 25°C

Components	Composition	$\bar{K}_a$[mJ/m^2]	κ[k_BT]	M_1[$\times 10^3$ s^{-1}]
POPC	100%	213 ± 5	38.5 ± 0.8	47.0 ± 0.5
Cholesterol	10%	240 ± 2	54.4 ± 1.2	57.0 ± 0.6
	20%	276 ± 5	70.2 ± 0.8	66.1 ± 0.7
	30%	354 ± 5	86.8 ± 1.4	75.0 ± 0.8
Lanosterol	10%	230 ± 4	51.7 ± 1.2	56.4 ± 0.3
	20%	260 ± 6	61.3 ± 1.1	61.7 ± 0.2
	30%	281 ± 6	71.5 ± 0.6	65.1 ± 0.2
Ergosterol	10%	216 ± 4	45.8 ± 1.1	51.5 ± 0.5
	20%	233 ± 7	53.5 ± 1.7	58.3 ± 0.6
	30%	241 ± 8	54.6 ± 1.1	57.6 ± 0.6

The area expansion modulus, $\bar{K}_a$, was determined by micropipette aspiration. Values of membrane bending rigidity, κ, were previously reported (33). The first moments, M_1, of the ^{2}H-NMR spectra were determined for sterols in POPC-d_{31} membranes. Values for cholesterol were interpolated from data previously reported (19). Error on κ and $\bar{K}_a$ represents standard deviation from the mean value of a population of vesicles. Lanosterol error represents standard deviation from the average of five scans each of 20,000 averages.

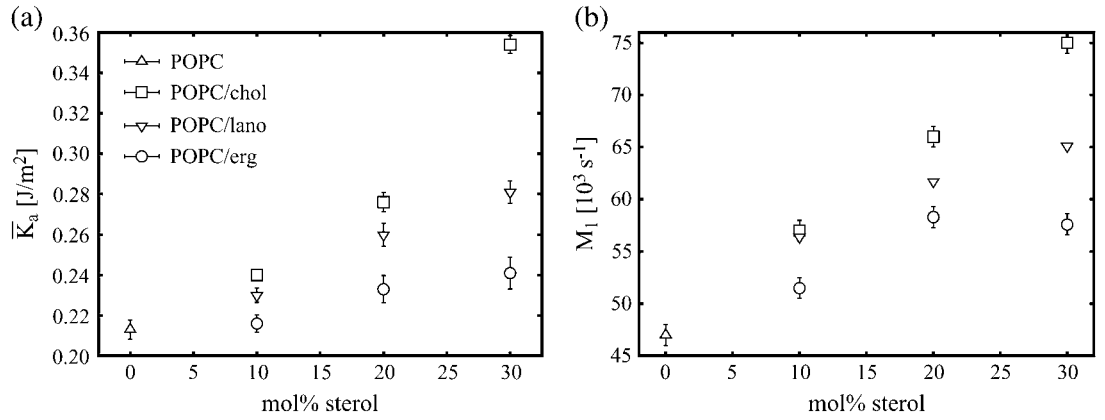

FIGURE 4 Plot of (*a*) the apparent area expansion modulus, $\bar{K}_a$ and (*b*) the first moment of the ^{2}H-NMR spectrum, M_1, as a function of sterol content. $\bar{K}_a$ is determined by micropipette aspiration and M_1 by ^{2}H-NMR. The extent to which these sterols increase $\bar{K}_a$ and M_1 follows the sequence cholesterol > lanosterol > ergosterol for all measured sterol concentrations. Numerical values and error are reported in Table 1.

^{2}H-NMR

^{2}H-NMR spectra were obtained for multilamellar dispersions of POPC-d_{31} containing 10, 20, and 30 mol% lanosterol and ergosterol at 25°C. The M_1 values for POPC-d_{31}/cholesterol were interpolated from data previously reported at 20 and 30°C (19). Fig. 5 shows spectra obtained for binary mixtures of POPC-d_{31} with lanosterol. The spectral width is observed to increase with sterol concentration. At a concentration of 30 mol% sterol, the average spectral width increases following the sequence cholesterol > lanosterol > ergosterol.

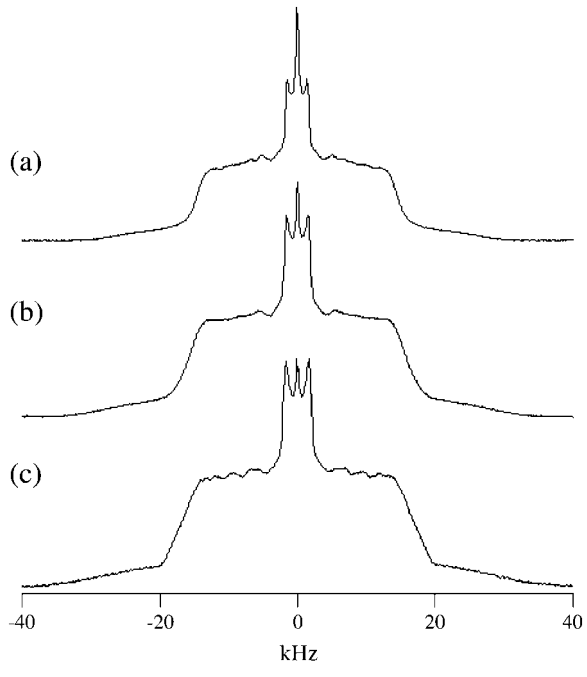

FIGURE 5 Spectra obtained by ^{2}H-NMR for POPC-d_{31} membranes containing (*a*) 10 mol%; (*b*) 20 mol%; and (*c*) 30 mol% lanosterol at 25°C. Acquisition parameters are documented in the text.

Increasing the concentration of a particular sterol species in POPC-d_{31} membranes results in an increase in the average width of the obtained spectra. To describe this effect quantitatively, the average spectral width is expressed as the first moment, M_1 (Eq. 5). M_1 values are determined for the acquired spectra and are displayed together with standard deviations in Table 1 and Fig. 4 *b*. As illustrated, the incorporation of these sterols into POPC-d_{31} membranes results in a progressive increase in M_1 with sterol content at 25°C. The extent to which the three sterols increase M_1 values follows the sequence cholesterol > lanosterol > ergosterol. For cholesterol and lanosterol, M_1 is nearly directly proportional to sterol concentration. The effect of ergosterol, however, is seen to plateau above 20 mol% ergosterol.

In the liquid crystalline phase, where acyl chains undergo rapid, axially symmetric reorientation about the bilayer normal, M_1 is proportional to the average order parameter. Thus, an increase in sterol concentration results in increased lipid acyl chain order. The relative increases in M_1 for 10, 20, and 30 mol% sterol with respect to the value of pure POPC-d_{31} are: 21%, 41%, and 60% for cholesterol; 20%, 31%, and 39% for lanosterol; and 10%, 24%, and 23% for ergosterol.

Discussion of data

Both micropipette aspiration and ^{2}H-NMR reveal these three sterols are membrane rigidifiers that order lipid acyl chains in POPC bilayers. The potency of their effects follows the sequence cholesterol > lanosterol > ergosterol. We observe the same qualitative behavior for both $\bar{K}_a$ and M_1 as a function of membrane sterol content (Fig. 4). For cholesterol and lanosterol, the effective increase in both $\bar{K}_a$ and M_1 is nearly linear with sterol concentration. For ergosterol, the increase levels off above 20 mol% ergosterol. A similar plateau effect of ergosterol has been observed using other techniques (23,44,45).

The results for $\bar{K}_a$ are in agreement with previous micropipette aspiration experiments showing that cholesterol

increases membrane stability (DPPC and SOPC) (30,36). Micropipette aspiration has also been used to determine the effects of lanosterol and ergosterol on DPPC membranes at low temperature (10°C) (13). In that study, the increase in the area expansion modulus was shown to follow the sequence ergosterol > cholesterol > lanosterol. This is not consistent with our observations of POPC membranes and indicates that sterols' sequential rigidifying effect on membranes is sensitive to lipid packing, for example, the nature of the lipid species (saturated versus unsaturated) and/or temperature relative to T_m. In both cases, it is clear that sterols promote membrane stability.

The effect of sterols on membrane mechanics can be understood in terms of how cholesterol, lanosterol, and ergosterol promote lipid acyl-chain order. Indeed, ^{2}H-NMR reveals that all three sterols induce an increase in the spectral width, M_1, with the same sequence as for the mechanical moduli. This observed increase in M_1 is consistent with previous NMR studies (19,22) and computer simulations (46,47) that show how sterols induce acyl-chain order in both saturated and unsaturated lipid bilayers. Some of these studies have revealed that cholesterol induces a larger increase in acyl-chain order parameters than lanosterol (12,14,23,27,46,48). Also with NMR, the interaction of sterols with lipid bilayers was found to be sensitive to the temperature relative to T_m (13,23).

These results are consistent with previous studies showing that the presence of sterols in membranes increases the membrane bending rigidity, κ (29,33,48,49). Correlating κ to $\bar{K}_a$ and M_1 sheds new light on the properties of membranes containing sterols. Fig. 6 *a* reveals that for a given value of κ there is a corresponding value of $\bar{K}_a$, which is independent of sterol type and concentration. Moreover, it is found that for a given sterol and concentration, the relative increase in κ is larger than that of $\bar{K}_a$. These sterols are thus more effective in rigidifying the membrane than increasing membrane resistance to area expansion.

Fig. 6 *b* illustrates how κ/K_a varies as a function of M_1. It has previously been demonstrated that the relation $\kappa/K_a \sim d^2$ holds for pure lipid membranes (38,50), which is consistent with simple shell theory. Considering that the hydrophobic thickness, d, increases linearly with M_1 (6,51), it follows that the shell model fails to describe the behavior of sterol-POPC lipid mixtures.

Further insights into the relationship between membrane mechanical properties and acyl-chain order are obtained by plotting the mechanical moduli versus M_1 (Fig. 7), revealing a remarkable data collapse. Fig. 7 illustrates that the dependence of $\bar{K}_a$ and κ on M_1 differs. Whereas $\bar{K}_a$ shows a parabolic form (Fig. 7 *a*), κ exhibits a nearly linear dependence on M_1 (Fig. 7 *b*). A previous study pursued a qualitative correlation of NMR and micropipette aspiration data for DPPC membranes containing 40% cholesterol, lanosterol, or ergosterol (13). In the present study, we have resolved the functional dependence of both κ and K_a on M_1 and sterol content.

At 25°C, POPC membranes are in the l_d phase. With increasing sterol concentration, we progress from the l_d to the l_o region in the phase diagram and acyl-chain order is observed to progressively increase. Previous investigations of cholesterol-POPC mixtures indicated $l_d - l_o$ phase separation in the range 5–30 mol% (20,52). Neither our micromechanical nor our NMR studies support the existence of macroscopic phase separation in this concentration range. Also, the spectra obtained by VFA are consistent with those of homogeneous liquid mixtures (33). We cannot exclude, however, the possibility of microphase separation or critical fluctuations due to the presence of a consulate point of a $l_d - l_o$ coexistence region.

Taken together, our results demonstrate that the mechanical properties of lipid membranes are governed primarily by the state of the lipid components. This indicates that sterols act to modify acyl-chain order, and in this way influence membrane mechanical properties. We further explore these findings in terms of simple theoretical considerations.

Theoretical considerations

In this section, we focus on how we can learn about fundamental sterol-lipid interactions by use of the experimental

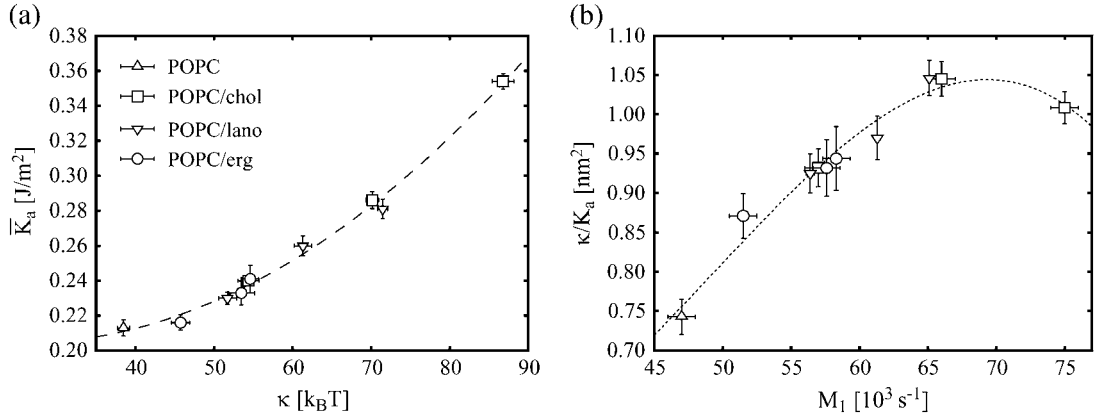

FIGURE 6 Plot of (*a*) the area expansion modulus, $\bar{K}_a$, as a function of the bending rigidity, κ, and (*b*) the ratio $\kappa/\bar{K}_a$ as a function of M_1.

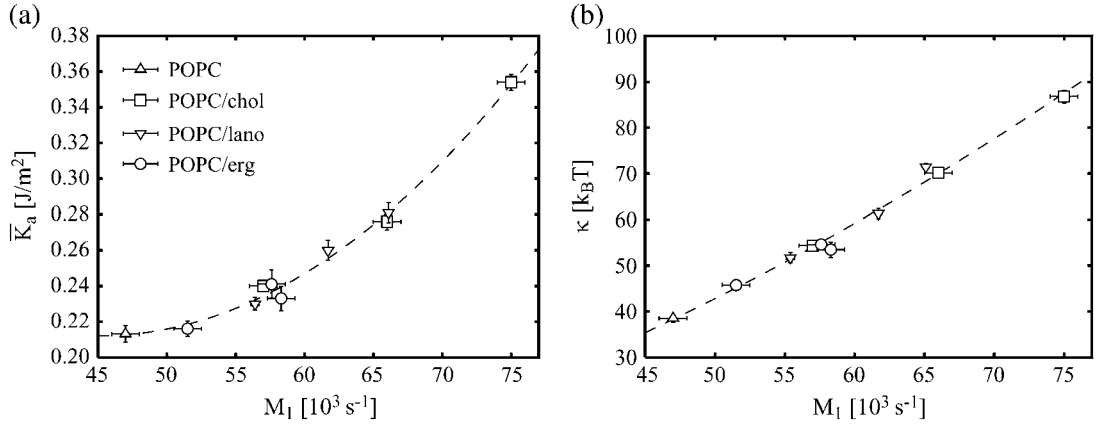

FIGURE 7 Plot of (*a*) the area expansion modulus, $\bar{K}_a$, and (*b*) the bending rigidity, κ, as a function of the acyl chain order measured by M_1. Both mechanical moduli exhibit a unique functional dependence on M_1 independently of sterol structure and concentration. Numerical values and error are reported in Table 1.

results and some minimal assumptions. Let us consider a monolayer of the membrane with N_l lipids and N_s sterols. The cross-sectional area of the sterols is considered as a constant ($\sim$32 Å^2). This is justified by the fact that sterols are rigid molecules that are not easily deformed in the lipid matrix (53). It follows that the canonical free energy is the relevant thermodynamic potential,

$$F(N_l, N_s, a_l, T) = Nf(x, a_l, T), \tag{7}$$

where $N = N_l + N_s$ is the total number of molecules and $x = (N_s/N)$ the mol fraction of sterols. As described above, the total area, $A = N_l a_l + N_s a_s$, is related to the lateral tension

$$\tau = \frac{\partial F}{\partial A}\Big)_{N_l,N_s,T} = \frac{\partial a_l}{\partial A}\Big)_{N_l,N_s,T}\frac{\partial F}{\partial a_l}\Big)_{N_l,N_s,T} = \frac{1}{1-x}\frac{\partial f}{\partial a_l}\Big)_{x,T}. \tag{8}$$

For a freestanding membrane in mechanical equilibrium, $\tau = 0$. The area expansion modulus is

$$K_a = A_o\frac{\partial \tau}{\partial A}\Big)_{N_l,N_s,T} = \frac{a_l^o(1-x) + a_s x}{1-x}\frac{\partial \tau}{\partial a_l})_{x,T}, \tag{9}$$

where A_0 is the total area and $a_l{}^0$ the lipid cross-sectional area in equilibrium. The experimentally determined correlation between lipid order (cross-sectional area) and area expansion modulus for all three mixtures shown in Fig. 7 can be expressed as $K_a(a_l, x) = K_a(a_l(x))$. In other words, there is no explicit x-dependence in K_a, so with the definitions in Eqs. 7–9 we get

$$\frac{\partial K_a}{\partial x}\Big)_{a_l,T} = 0 \Rightarrow f(x, a_l) = \frac{1-x}{a_l^o + a_s\frac{x}{1-x}}(U(x)a_l + V(a_l)) + W(x). \tag{10}$$

$U(x)$, $V(a_l)$, and $W(x)$ are some general differentiable functions to be determined, where some properties of U and V are obtained from the experimental results (note that W may contain contributions from interactions between sterols and entropy of mixing). The first term represents contributions to the chemical potential of the lipids. The term U encompasses the interfacial tension and the interaction between lipid and sterol molecules. Contributions to V can derive from, for example, chain conformational energy, the entropy confinement of floppy lipid chains, and Flory-Huggins-like entropy of mixing. In this representation, the equilibrium condition is $V'(a_l) = -U(x)$ and the area expansion modulus $K_a = V''(a_l)$. To establish the connection between membrane mechanical properties and acyl-chain order, we note that the average order parameter, $\langle|S_{CD}|\rangle$, is affinely related to the bilayer's hydrophobic thickness, d, (15,51,54). Hence, M_1 values provide a simple way of estimating bilayer hydrophobic thickness and cross-sectional areas by use of hydrophobic volume conservation, $(a_o)/(a_l) = (d)/(d^0) = 1+\tilde{\alpha}m$, where $m = M_1 - M_1^0$ and M_1^0 is M_1 for pure POPC-d_{31} (Table 1). We will use the estimated values of the hydrophobic thickness $d^0 = 25.8$ Å for pure POPC-d_{31} at 25°C (54) on the basis of theory and data from x-ray diffraction and ^{2}H-NMR. The constant $\tilde{\alpha}$ is calibrated to 5.8×10^{-6} s within 10% error from values reported in Table 1 and Nezil and Bloom (54) for cholesterol-POPC-d$_{31}$ mixtures.

The correlation between the experimental data for $\bar{K}_a$ and M_1 (Table 1 and Fig. 7) can be parameterized by a Taylor expansion. Following from the above considerations, this relation can also be established for theoretical potentials

$$\frac{K_a(a_l) - K_a(a_l^o)}{K_a(a_l^o)} = \sum_{i=1}^{n} g_i m^i + O(\tilde{\alpha}^{n+1}m^{n+1}). \tag{11}$$

The coefficients g_i depend on $\tilde{\alpha}$ and the particular form of $V(a_l)$. The experimentally determined values are $g_1^{ex} = 3.9 \times 10^{-7}$ s, $g_2^{ex} = 1.9 \times 10^{-10}$ s^2, and $g_3^{ex} = 1.0 \times 10^{-19}$ s^3. This shows that the second-order term is the most significant, whereas higher-order terms are negligible. The observed behavior cannot be captured by simple phenomenological potentials used in the literature, e.g., the form

$V(a_l) = \gamma a_l + \xi/a_l$, that accounts for interfacial tension and phospholipid headgroup repulsion (55). In the absence of a good model underlying the behavior of V, we can parameterize the potential using the experimental quantity m from integration of Eq. 11.

Now, let us turn to the form of $U(x)$. To get a picture of the contributions to U we Taylor-expand to second-order in x,

$$U(x) = u_0 + u_1 x + u_2 x^2. \tag{12}$$

Here u_0 determines the equilibrium condition $V'(a_l^0) = -u_0$ for pure POPC, so this term has the character of an interfacial tension. The second term has the form of enthalpy of mixing for pair interactions between lipid and sterol, and the third term is relevant if multibody effects are of importance in the system.

The equilibrium condition can now be investigated for V',

$$V'(a_l) = \int_{a_l^0}^{a_l} \mathrm{d}a V''(a) = -a_l^0 V''(a_l^0) \times \int_0^{m(a)} \frac{g_1^{exp} m' + g_2^{exp} m'^2 + \cdots}{(1+\tilde{\alpha}m')^2} \mathrm{d}m', \tag{13}$$

where we set $V'(a_l^0) = 0$ (the $u_0 a_l$ term is included in V). Expanding Eq. 13 in m to cubic order, the equilibrium condition is

$$u_1 x + u_2 x^2 = K_a(a_l^0) a_l^0 \tilde{\alpha} \left[m + \left(\frac{1}{2} g_1^{exp} - \tilde{\alpha} \right) m^2 + \left(\tilde{\alpha}^2 + \frac{1}{3} g_2^{exp} - \frac{2}{3} g_1^{exp} \tilde{\alpha} \right) m^3 \right]. \tag{14}$$

Based on the experimental data, the parameters u_1 and u_2 can now be calculated for each sterol. A simple fit gives $(u_1, u_2)_{cholesterol} = (8, -3)k_BT$, $(u_1, u_2)_{lanosterol} = (8, -13)k_BT$, and $(u_1, u_2)_{ergosterol} = (9, -12)k_BT$ where error is estimated to be on the order of 10% and 25% for u_1 and u_2, respectively. These findings suggest that contributions from pair interactions vary little between the sterols whereas multibody effects (packing) differ significantly between cholesterol, lanosterol, and ergosterol. Note that the results for ergosterol differ if a saturation limit of this sterol in the membrane is attained.

For the bending rigidity a similar data collapse is observed, $\kappa(a_l, x) = \kappa(a_l(x))$ or $(\partial\kappa)/(\partial \mathrm{x})\big)_{a_l} = 0$. Following the same procedure as above, assuming bilayer symmetry, and expanding the free energy in the mean curvature around the flat configuration $H = 0$, the data collapse implies that

$$\frac{F}{A} = \frac{\kappa(a_l)}{2}(2H)^2 + \bar{f}(a_l, x, H = 0), \tag{15}$$

where $\bar{f}(a_l, x, H = 0)$ is dealt with above (Eq. 10), and Fig. 7*b* contains information about the functional form of $\kappa(a_l)$. Various models for the bending rigidity have been introduced which predict that $\kappa \propto d^{\nu}/a^{\mu}_{mol}$ (50,56), where a_{mol} is some characteristic molecular area. From Eq. 15, it is clear that this can only be the lipid cross-sectional area, a_l. Formulating this class of relationships in terms of first-moments yields

$$\frac{\kappa(M_1) - \kappa(M_1^0)}{\kappa(M_1^0)} = (1 + \tilde{\alpha}m)^{\nu+\mu}. \tag{16}$$

Fitting the form in Eq. 16 to the experimental results shown in Fig. 7 *b* yields $\nu + \mu = 5.6 \pm 1.1$. It is interesting to note that a simple random coil and packing model of lipid chains predicts $\nu + \mu = 5$ (56).

DISCUSSION AND CONCLUSION

Our study demonstrates that for POPC-sterol mixtures, lipid chain order determines membrane mechanical properties. Although the relative effects differ for each sterol, the observed data collapse signals some universal features of these sterol-lipid systems expressed through relations between the elastic moduli and first moments of ^{2}H-NMR spectra. Such behavior may be the underlying reason for the remarkable robustness of the phase diagram topology for lipid-cholesterol mixtures observed for a range of saturated and monounsaturated lipids (11,17,21,52). The strong similarity between sterols' effects on lipid membranes was also described in a previous study (27) where only minor changes in a statistical mechanical model were needed to account for the differences in order parameters and phase behavior observed by ^{2}H-NMR in mixtures of 1-palmitoyl-2-petroselinoyl-*sn*-glycero-3-phosphatidylcholine with cholesterol and lanosterol. The universal behavior observed in this study can also be correlated with another universal relationship obtained for lipid systems by ^{2}H-NMR (26,57), which can be restated as follows: for a given deuterated lipid chain exposed to some perturbation, there is a universal set of order parameter profiles $S_{CD}(n)$, that depends only on $\langle|S_{CD}|\rangle$ and is independent of the origin of the chain perturbation whether this be headgroup, temperature, and/or sterol content. This finding establishes a one-to-one correspondence between the family of order profiles, parameterized by $\langle|S_{CD}|\rangle$, and K_a, which depends only on M_1 or $\langle|S_{CD}|\rangle$ through the potential, V, at fixed temperature. Our results for varying sterol content in POPC membranes at room temperature thus confirm the conjecture that there is a close relationship between the order parameter profile and membrane elastic behavior (6). Order parameters reflect acyl-chain conformational entropy, thus the structure and flexibility of lipid chains under constrained conditions appears to be the natural origin of both the shape of $S_{CD}(n)$ as well as the potential V that describes K_a. The connection of our results to the universality of order parameter profiles makes it natural in future work to extend the analysis into the temperature domain.

The factors that perturb lipid chain order, and thus membrane mechanical properties, are contained in the generalized surface tension $U(x)$ that captures the complex interaction between sterols and lipids. In particular, the potency to order

the acyl chain is contained in U such that $U_{\text{ergosterol}} < U_{\text{lanosterol}} < U_{\text{cholesterol}}$. Our results showing that effective multibody interactions play a major role in sterol-lipid interactions indicate that the effect of packing in membrane-sterol behavior is significant. This is in accordance with the established view (9,10,58). Note that the potency of acyl chain ordering depends on the nature of the acyl chains (13,23,33).

Differences in the relative effects of sterols on membrane packing and properties can be attributed to small differences in sterol structure. With three additional methyl groups, lanosterol is a bulkier molecule than cholesterol. The shedding of lanosterol's methyl groups in the biosynthetic pathway gives rise to cholesterol, whose smoother structure may facilitate stronger cohesive interactions with lipids than its synthetic precursor, lanosterol (27). Structurally, ergosterol differs from cholesterol in that it has two additional double bonds as well as a methyl group on the side chain.

These subtle structural variations can give rise to differences in the effect of sterols on membrane properties. For example, sterols influence the state of hydration in the headgroup region (1): the penetration of water into POPC lipid bilayers has been shown by fluorescence techniques to vary between cholesterol, lanosterol, and ergosterol (14,44). Also, different sterols alter the membrane permeability barrier to varying extents (59), and in general reduce the membrane-partitioning of exogenous compounds such as alcohols (1,60). It is unclear if these effects are a consequence of, or are caused by, altered interactions in the headgroup region.

One may question the implications of differences in sterol structure for biological function. Although sterols seem to universally promote the lateral membrane heterogeneity that is important for biological function (reviewed in (1,2,61)), the formation and stability of domains in membranes varies depending on sterol structure (62–65). Also, the action of polyene antibiotics (amphotericin B) has been shown to be much more active in ergosterol-containing membranes (66,67). The different effects of cholesterol and ergosterol could represent evolutionary divergence from their biosynthetic precursor, lanosterol.

Here we have shown that small differences in sterol structure give rise to marked alterations in membrane properties. Nonetheless, this study indicates that, although the relative effects of cholesterol, lanosterol, and ergosterol on membrane thickness and sterol-lipid packing may differ, the way in which these sterols modify membrane hydrophobic thickness and elastic properties is universal.

APPENDIX

Even at high tension levels membrane undulations persist. This renormalizes the area expansion modulus. To evaluate the magnitude of this correction, Eq. 57 in Henriksen and Ipsen (37) is expanded to lowest order in $K_a/(\kappa\beta\tau)$:

$$\bar{K}_a(\tau) \simeq K_a\left(1 - \frac{K_a}{8\pi\kappa\beta\tau} + \mathcal{O}\left(\frac{K_a}{\kappa\beta\tau}\right)^{!!2}\right). \qquad (17)$$

Typically, K_a is acquired by fitting data in a specific tension range $[\tau_{\min};\tau_{\max}]$. The correction from thermal renormalization is obtained as an average over this particular tension range

$$\begin{aligned}\bar{K}_a &= (\tau_{\max} - \tau_{\min})^{-1}\int_{\tau_{\min}}^{\tau_{\max}} \bar{K}_a\tau)\,\mathrm{d}\tau \\ &= K_a\left(1 - \frac{K_a \ln(\tau_{\max}/\tau_{\min})}{8\pi\kappa\beta(\tau_{\max} - \tau_{\min})}\right). \qquad (18)\end{aligned}$$

If κ and K_a are known, Eq. 18 can be applied to estimate the reduction of K_a for a given τ-fitting range. For these particular sterol-lipid systems, the relative reduction of the apparent area expansion modulus, $(\bar{K}_a/K_a - 1)$, is estimated to be 3–7%. This estimate is based on κ- and K_a-values for the pure POPC lipid membrane as reported in Table 1 and the tension range $\tau \in [2;x]$ mN/m, $x \geq 5$. The relative reduction is generally proportional to K_a/κ and declines as a function of $\tau_{\min}$ and $\tau_{\max}$.

Thanks to John Cheng for his skillful lab work. The authors also thank Myer Bloom, a great source of sterol inspiration.

MEMPHYS - Centre for Membrane Biophysics is supported by the Danish National Research Foundation. A.C.R. is supported by a Julie Payette Scholarship from the National Research Council of Canada. Y.H. received support from National Science Council of Taiwan (grant No. NSC 92-2112-M-008-049).

REFERENCES

1. Barenholz, Y. 2004. Sphingomyelin and cholesterol: from membrane biophysics and rafts to potential medical applications. *In* Subcellular Biochemistry. P.J. Quinn, editor. Kluwer Academic/Plenum, New York. 167–215.
2. Simons, K., and W. L. C. Vaz. 2004. Model systems, lipid rafts, and cell membranes. *Annu. Rev. Biophys. Biomol. Struct.* 33:269–295.
3. Bloch, K. 1976. On the evolution of a biosynthetic pathway. *In* Reflections on Biochemistry. A. Kornberg, B.L. Horecker, L. Cornudella, and J. Orci, editors. Pergamon Press, New York. 143–150.
4. Bloch, K. E. 1983. Sterol structure and membrane function. *CRC Crit. Rev. Biochem.* 19:47–92.
5. Nes, W. R. 1974. Role of sterols in membranes. *Lipids*. 9:596–612.
6. Bloom, V., E. Evans, and O. G. Mouritsen. 1991. Physical properties of the fluid lipid-bilayer component of cell membranes: a perspective. *Q. Rev. Biophys.* 24:293–397.
7. Yeagle, P. L. 1985. Lanosterol and cholesterol have different effects on phospholipid acyl chain ordering. *Biochim. Biophys. Acta*. 815:33–36.
8. Finegold, L., Editor. 1993. Cholesterol in Membrane Models. CRC Press, Boca Raton, FL.
9. Presti, F. T. 1985. The role of cholesterol in membrane fluidity. *In* Membrane Fluidity in Biology: Cellular Aspects, Vol. 4. R.C. Aloia and J.H. Boggs, editors. Academic Press, New York. 97–106.
10. Ipsen, J. H., G. Karlström, O. G. Mouritsen, H. Wennerström, and M. J. Zuckermann. 1987. Phase equilbria in the phosphatidylcholine-cholesterol system. *Biochim. Biophys. Acta*. 905:162–172.
11. Vist, M. R., and J. H. Davis. 1990. Phase-equilibria of cholesterol dipalmitoylphosphatidylcholine mixtures—H-2 nuclear magnetic resonance and differential scanning calorimetry. *Biochemistry*. 29:451–464.
12. Nielsen, M., J. Thewalt, L. Miao, J. H. Ipsen, M. Bloom, M. J. Zuckermann, and O. G. Mouritsen. 2000. Sterol evolution and the physics of membranes. *Europhys. Lett.* 52:368–374.
13. Endress, E., S. Bayerl, K. Prechtel, C. Maier, R. Merkel, and T. M. Bayerl. 2002. The effect of cholesterol, lanosterol and ergosterol on lecithin bilayer mechanical properties at molecular and microscopic dimensions: a solid-state NMR and micropipette study. *Langmuir*. 18:3293–3299.

14. Huster, D., H. A. Scheidt, K. Arnold, A. Herrmann, and P. Müller. 2004. Desmosterol may replace cholesterol in lipid membranes. *Biophys. J.* 88:1838–1844.

15. Ipsen, J. H., O. G. Mouritsen, and M. Bloom. 1990. Relationships between lipid membrane area, hydrophobic thickness, and acyl-chain orientational order: the effects of cholesterol. *Biophys. J.* 57:405–412.

16. Finegold, L., and M. A. Singer. 1993. Cholesterol/phospholipid interactions studied by differential scanning calorimetry: effect of acyl chain length and role of the C(17) sterol side group. *In* Cholesterol in Membrane Models. L. Finegold, editor. CRC Press, Boca Raton, FL. 137–157.

17. Almeida, P. F. F., W. L. C. Vaz, and T. E. Thompson. 1992. Lateral diffusion in the liquid phases of dimyristoylphosphatidylcholine/cholesterol lipid bilayers. *Biochemistry.* 31:6739–6747.

18. Linseisen, F. M., J. L. Thewalt, M. Bloom, and T. M. Bayerl. 1993. ^{2}H-NMR and DSC study of SEPC-cholesterol mixtures. *Chem. Phys. Lipids.* 65:141–149.

19. Thewalt, J. L., C. E. Hanert, F. M. Linseisen, A. J. Farrall, and M. Bloom. 1992. Lipid-sterol interactions and the physical properties of membranes. *Acta Pharm.* 42:9–23.

20. Rappolt, M., M. F. Vidal, M. Kriechbaum, M. Stienhert, H. Amentisch, S. Bernstorff, and P. Laggner. 2003. Structural, dynamic, and mechanical properties of POPC at low cholesterol concentration studied in pressure/temperature space. *Eur. Biophys. J.* 31:575–585.

21. Thewalt, J. L., and M. Bloom. 1992. Phosphatidylcholine/cholesterol phase diagrams. *Biophys. J.* 63:1176–1181.

22. Hsueh, Y. W., K. Gilbert, C. Trandum, M. Zuckermann, and J. Thewalt. 2005. The effect of ergosterol on dipalmitoylphosphatidylcholine bilayers: a deuterium NMR and calorimetric study. *Biophys. J.* 88:1799–1808.

23. Urbina, J. A., S. Pekerar, H. Le, J. Patterson, B. Montez, and E. Oldfield. 1995. Molecular order and dynamics of phosphatidylcholine bilayer membranes in the presence of cholesterol, ergosterol and lanosterol: a comparative study using ^{2}H-, ^{13}C- and ^{31}P-NMR spectroscopy. *Biochim. Biophys. Acta.* 1238:163–167.

24. Endress, E., H. Heller, H. Casalta, M. F. Brown, and T. M. Bayerl. 2002. Anisotropic motion and molecular dynamics of cholesterol, lanosterol, and ergosterol in lecithin bilayers studied by quasi-elastic neutron scattering. *Biochemistry.* 41:13078–13086.

25. Jacobs, R., and E. Oldfield. 1979. Deuterium nuclear magnetic resonance investigation of dimyristoyllecithin-dipalmitoyllecithin and dimyristoyllecithin-cholesterol mixtures. *Biochemistry.* 18:3280–3285.

26. Lafleur, M., M. Bloom, and P. R. Cullis. 1991. Lipid polymorphism and hydrocarbon order. *Biochem. Cell Biol.* 68:1–8.

27. Miao, L., M. Nielsen, J. Thewalt, J. H. Ipsen, M. Bloom, M. J. Zuckermann, and O. G. Mouritsen. 2002. From lanosterol to cholesterol: structural evolution and differential effects on lipid bilayers. *Biophys. J.* 82:1429–1444.

28. Needham, D., T. J. McIntosh, and E. Evans. 1988. Thermomechanical and transition properties of dimyristoylphosphatidylcholine/cholesterol bilayers. *Biochemistry.* 27:4668–4673.

29. Patty, P. J., and B. J. Frisken. 2003. The pressure-dependence of the size of extruded vesicles. *Biophys. J.* 85:996–1004.

30. Needham, D., and R. S. Nunn. 1990. Elastic deformation and failure of lipid bilayer membranes containing cholesterol. *Biophys. J.* 58:997–1009.

31. Méléard, P., C. Gerbeaud, T. Pott, L. Fernandez-Puente, I. Bivas, M. D. Mitov, J. Dufourcq, and J. Bothorel. 1997. Bending elasticities of model membranes: influence of temperature and sterol content. *Biophys. J.* 72:2616–2629.

32. Duwe, H. P., J. Kaes, and E. Sackmann. 1990. Bending elastic moduli of lipid bilayers: modulation by solutes. *J. Phys. France.* 51:945–962.

33. Henriksen, J. R., A. C. Rowat, and J. H. Ipsen. 2004. Vesicle fluctuation analysis of the effects of sterols on membrane bending rigidity. *Eur. Biophys. J.* 33:732–741.

34. Helfrich, W. 1973. Elastic properties of lipid bilayers: theory and possible experiments. *Z. Naturforsch.* 28:693–703.

35. Kim, D. H., and D. Needham. 2002. Lipid bilayers and monolayers: characterization using micropipette manipulation techniques. *In* Encyclopedia of Surface and Colloid Science. A. Hubbard, editor. Marcel Dekker, New York. 3057–3086.

36. Evans, E., and W. Rawicz. 1990. Entropy-driven tension and bending elasticity in condensed-fluid membranes. *Phys. Rev. Lett.* 64:2094–2097.

37. Henriksen, J. R., and J. H. Ipsen. 2004. Measurement of membrane elasticity by micro-pipette aspiration. *Eur. Phys. J. E.* 14:149–167.

38. Rawicz, W., K. C. Olbrich, T. McIntosh, D. Needham, and E. Evans. 2000. Effect of chain length and unsaturation on elasticity of lipid bilayers. *Biophys. J.* 79:328–339.

39. Henriksen, J. R., and J. H. Ipsen. 2002. Thermal undulations of quasi-spherical vesicles stabilized by gravity. *Eur. Phys. J.* 9:365–374.

40. Angelova, M. I., and D. S. Dimitrov. 1986. Liposome electroformation. *Faraday Discuss. Chem. Soc.* 81:303–311.

41. Angelova, M. I., S. Soléau, P. Méléard, J. F. Faucon, and P. Bothorel. 1992. Preparation of giant vesicles by external AC electric fields. Kinetics and applications. *Prog. Colloid Polym. Sci.* 89:127–131.

42. Backer, J. M., and E. A. Dawidowicz. 1981. Transmembrane movement of cholesterol in small unilamellar vesicles detected by cholesterol oxidase. *J. Biol. Chem.* 256:586–588.

43. Davis, J. H., K. R. Jeffrey, M. Bloom, M. I. Valic, and T. P. Higgs. 1976. Quadrupolar echo deuteron magnetic resonance spectroscopy in ordered hydrocarbon chains. *Chem. Phys. Lett.* 42:3390–3394.

44. Arora, A., H. Raghuraman, and A. Chattopadhyay. 2004. Influence of cholesterol and ergosterol on membrane dynamics: a fluorescence approach. *Biochem. Biophys. Res. Commun.* 318:920–926.

45. Semer, R., and E. Gerelinter. 1979. A spin label study of the effects of sterols on egg lecithin bilayers. *Chem. Phys. Lipids.* 23:201–211.

46. Smondyrev, A. M., and M. L. Berkowitz. 2001. Molecular dynamics simulation of the structure of dimyristoylphosphatidylcholine bilayers with cholesterol, ergosterol, and lanosterol. *Biophys. J.* 80:1649–1658.

47. Hofsäss, C., E. Lindahl, and O. Edholm. 2003. Molecular dynamics simulations of phospholipid bilayers with cholesterol. *Biophys. J.* 84: 2192–2206.

48. Martinez, G. V., E. M. Dykstra, S. Lope-Piedrafita, and M. F. Brown. 2004. Lanosterol and cholesterol-induced variations in bilayer elasticity probed by ^{2}H-NMR relaxation. *Langmuir.* 20:1043–1046.

49. Petrache, H. I., D. Harries, and V. A. Parsegian. 2005. Alteration of lipid membrane rigidity by cholesterol and its metabolic precursors. *Macromol. Symp.* 219:39–50.

50. Fernandez-Puente, L., I. Bivas, M. D. Mitov, and P. Méléard. 1994. Temperature and chain length effects on bending elasticity of phosphatidylcholine bilayers. *Europhys. Lett.* 28:181–186.

51. Schindler, H., and J. Seelig. 1975. Deuterium order parameters in relation to thermodynamic properties of a phospholipid bilayers. A statistical mechanical interpretation. *Biochemistry.* 14:2283–2287.

52. Mateo, C. R., A. V. Acu, A. Tilden, and T. C. Brochon. 1995. Liquid-crystalline phases of cholesterol/lipid bilayers as revealed by the fluorescence of *trans*-parinaric acid. *Biophys. J.* 68:978–987.

53. Ghosh, D., and J. Tinoco. 1972. Monolayer interactions of individual lecithins with natural sterols. *Biochim. Biophys. Acta.* 266:41–49.

54. Nezil, F. A., and M. Bloom. 1992. Combined influence of cholesterol and synthetic and amphiphilic polypeptides upon bilayer thickness in model membranes. *Biophys. J.* 61:1176–1183.

55. Israelachvili, J. N., D. J. Mitchell, and B. W. Ninham. 1976. Theory of self-assembly of hydrocarbon amphiphiles into micelles and bilayers. *J. Chem. Soc. Faraday Trans. II.* 72:1525–1568.

56. Gelbart, W. M., and A. Ben-Shaul. 1987. Chain packing and the compressional elasticity of surfactant films. *In* Physics of Amphiphilic Layers. J. Meunier, D. Langevin, and N. Boccara, editors. Springer-Verlag, Heidelberg, Germany. 9–12.

57. Morrow, M. R., and D. Lu. 1991. Universal behaviour of lipid acyl chain order: chain length scaling. *Chem. Phys. Lett.* 182:435–439.

58. Scott, M. L. 1991. Lipid-cholesterol interactions: Monte Carlo simulations and theory. *Biophys. J.* 59:445–455.

59. Demel, R. A., K. R. Bruckdorfer, and L. L. M. van Deenen. 1972. The effect of sterol structure on the permeability of liposomes to glucose, glycerol, and Rb^+. *Biochim. Biophys. Acta.* 255:321–330.

60. Trandum, C., P. Westh, K. Jørgensen, and O. G. Mouritsen. 2000. A thermodynamic study of the effects of cholesterol on the interaction between liposomes and ethanol. *Biophys. J.* 78:2486–2492.

61. Helms, J. B., and C. Zurzolo. 2004. Lipids as targeting signals: lipid rafts and intracellular trafficking. *Traffic.* 5:247–254.

62. Xu, X., and E. London. 2000. The effect of sterol structure on membrane lipid domains reveals how cholesterol can induce lipid domain formation. *Biochemistry.* 39:843–849.

63. Xu, X., R. Bittman, G. Duportail, D. Heissler, C. Vilcheze, and E. London. 2001. Effect of the structure of natural sterols and sphingolipids on the formation of ordered sphingolipid/sterol domains (rafts). *J. Biol. Chem.* 276:33540–33546.

64. Wang, J., L. E. Megha, and E. London. 2004. Relationship between sterol/steroid structure and participation in ordered lipid domains (lipid rafts): implications for lipid raft structure and function. *Biochemistry.* 43:1010–1018.

65. Scheidt, H. A., P. Muller, A. Herrmann, and D. Huster. 2003. The potential of fluorescent and spin-labeled steroid analogs to mimic natural cholesterol. *J. Biol. Chem.* 278:45563–45569.

66. Bolard, J. 1986. How do polyene macrolide antibiotics affect the cellular membrane properties? *Biochim. Biophys. Acta.* 864:257–304.

67. Brajtburg, J., W. G. Powderly, G. S. Kobayashi, and G. Medoff. 1990. Amphotericin B: current understanding of mechanisms of action. *Antimicrob. Agents Chemother.* 34:183–188.